Journal of Photonics for Energy

SPIEDigitalLibrary.org/jpe

Optical properties of boride ultrahigh-temperature ceramics for solar thermal absorbers

Elisa Sani
Marco Meucci
Luca Mercatelli
David Jafrancesco
Jean-Louis Sans
Laura Silvestroni
Diletta Sciti

Optical properties of boride ultrahigh-temperature ceramics for solar thermal absorbers

Elisa Sani,[a,*] Marco Meucci,[a] Luca Mercatelli,[a] David Jafrancesco,[a] Jean-Louis Sans,[b] Laura Silvestroni,[c] and Diletta Sciti[c]

[a]CNR-INO, Istituto Nazionale di Ottica, Firenze 50125, Italy
[b]PROMES-CNRS Processes, Materials and Solar Energy Laboratory, Font Romeu 66120, France
[c]CNR-ISTEC, Istituto di Scienza e Tecnologia dei Materiali Ceramici, 48018 Faenza, Italy

Abstract. It is a known rule that the efficiency of thermodynamic solar plants increases with the working temperature. At present, the main limit in temperature upscaling is the absorber capability to withstand high temperatures. The ideal solar absorber works at high temperatures and has both a low thermal emissivity and a high absorptivity in the solar spectral range. The present work reports on the preparation and optical characterization of hafnium and zirconium diboride ultrahigh-temperature ceramics for innovative solar absorbers operating at high temperature. Spectral hemispherical reflectance from the ultraviolet to the mid-infrared wavelength region and high-temperature hemispherical emittance reveal their potential for high-temperature solar applications. Boride samples are compared with silicon carbide (SiC), a material already used in solar furnaces. © *2014 Society of Photo-Optical Instrumentation Engineers (SPIE)* [DOI: 10.1117/1.JPE.4.045599]

Keywords: optical properties; reflectance; emittance; borides; ultrahigh-temperature ceramics; concentrating solar power.

Paper 13044 received Dec. 20, 2013; revised manuscript received Jan. 13, 2014; accepted for publication Jan. 24, 2014; published online Feb. 18, 2014.

1 Introduction

Concentrating solar power (CSP) is one of the most promising technologies for electricity production in the future. As it is a general rule that the efficiency of solar thermal systems rapidly increases with increasing working temperature, there is a large effort to increase the operating temperatures (at present limited to <900 K) by developing novel solutions. For solar tower approach, a critical parameter is the material that constitutes the receiver, namely the absorber, where the heliostat field concentrates the collected sunlight. The ideal sunlight absorber material should have, at the same time, good optical properties (spectral selectivity against the thermal radiation, with a low reflectance at the solar spectrum wavelengths, and a high reflectance for longer wavelengths arising in a low thermal emittance) and favorable mechanical and thermal characteristics. Graphite (C), alumina (Al_2O_3), and silicon carbide (SiC) have been studied for solar receivers but they show serious drawbacks for significant operating temperature increases. Diborides and carbides of transition metals, such as zirconium boride (ZrB_2), hafnium boride (HfB_2), zirconium carbide (ZrC), and hafnium carbide (HfC), are commonly referred to as ultrahigh-temperature ceramics (UHTCs) for their extremely high melting temperatures exceeding 3000°C. Moreover, they show other favorable characteristics, such as good thermochemical and thermomechanical properties and high electrical and thermal conductivities.[1] UHTCs are ideal for thermal protection systems, especially those requiring chemical and structural stability at extremely high operating temperatures. In the framework of CSP sunlight exploitation, the favorable characteristics of UHTCs appear interesting for employing them in high-temperature novel solar furnaces, once the relevant optical properties have been assessed. Very recently, we studied UHTC samples consisting of ZrC and HfC obtaining both a good spectral selectivity and a low

*Address all correspondence to: Elisa Sani, E-mail: elisa.sani@ino.it

high-temperature emittance with respect to SiC.[2–4] In this work, we report on the comparative optical characterization of ZrB_2 and HfB_2 dense samples, in the perspective to evaluate the material potential as novel high-temperature solar absorber. We measured the room-temperature hemispherical reflectance spectra from the ultraviolet to the mid-infrared wavelength regions, comparing the boride spectral properties with those of a monolithic SiC. Moreover, we measured the boride hemispherical emittance in the wavelength range from 0.6 to 40 μm and in different spectral bands for temperatures ranging from 1100 to 1400 K.

2 Materials and Methods

Ceramics were prepared starting from commercial powders. Dense ZrB_2 and HfB_2 samples were prepared with $MoSi_2$ as sintering aid, with a typical content of 5 to 10 vol%. The powder mixtures were milled in absolute ethanol using ceramic milling media, subsequently dried in a rotary evaporator and sieved through a 250-μm screen. Further details on materials' preparation are available in Refs. 5–9. Samples constituted by monolithic SiC were also produced for reference. The mean surface roughness (R_a) was measured according to the European standard CEN 624-4 using a commercial contact stylus instrument (Taylor Hobson mod. Talysurf Plus, Leicester, UK) fitted with a 2-μm-radius conical diamond tip over a track length of 8 mm and with a cutoff length of 0.8 mm.

Optical hemispherical reflectance spectra in 0.25- to 2.5-μm wavelength region were acquired using a double-beam spectrophotometer (Lambda900 by Perkin Elmer, Waltham, MA) equipped with a 150-mm diameter Spectralon®-coated integration sphere for the measurement of the hemispherical reflectance. The spectra in the wavelength region 2.5 to 14.3 μm have been acquired using a Fourier transform spectrophotometer (FT-IR "Excalibur" by Bio-Rad, Hercules, California) equipped with a gold-coated integrating sphere and a liquid nitrogen-cooled detector. In all cases, the hemispherical reflectance spectra are acquired for quasi-normal incidence.

High-temperature hemispherical emittance has been measured using the Moyen d'Essai et de Diagnostic en Ambiance Spatiale Extreme (MEDIASE) setup developed at PROMES-CNRS laboratory.[10–12] MEDIASE is composed by a vacuum chamber with ultimate pressure limit of 10^6 mbar equipped with a hemispherical silica glass window of 35-cm diameter. The water-cooled sample holder is set to keep the specimen at the focus of the 1-MW solar furnace. Care is taken in mounting the sample in such a way as to minimize the thermal losses toward the holder. The flux incident on the sample is controlled both by a suitable choice of the mirrored area for sunlight capture and by adjusting a variable aperture door in front of the chamber. Directional radiance was measured on the rear face of the sample at different angles thanks to a movable, computer-controlled three-mirror system, using a radiometer as light detector. The acquired wavelength ranges are 0.6 to 40, 0.6 to 2.8, and 8 to 14 μm. The spectral response of the whole optical system was calibrated against a reference blackbody.

3 Results

An example of microstructural details of the samples under investigation is illustrated in Fig. 1 for HfB_2. To obtain an almost fully dense HfB_2 (99% density) the addition of 3 to 5 vol% of $MoSi_2$ and sintering temperature 1900°C are needed. X-ray diffraction analysis on the obtained sample is detected only with HfB_2, along with small traces of HfO_2 and SiC, with no $MoSi_2$ residuals due to the conversion of the silicide into SiC.[8]

As for ZrB_2, full density in the sample require a 5 to 10 vol% amount of $MoSi_2$ in the starting powders, and a sintering temperature of 1850°C. The final volumetric amount of $MoSi_2$ is slightly lower than starting composition due to the reaction during sintering arising in the formation of MoB and Mo-Si-B mixed phases, with a total amount of 1 to 2 vol%.

For reference, a SiC sample was also obtained by sintering at 1800°C, with a small percentage of alumina and yttria as sintering aids. Table 1 summarizes the investigated samples.

The room-temperature hemispherical reflectance spectra of dense ZrB_2 and HfB_2 samples are shown in Fig. 2 for polished samples. Borides are characterized by a high reflectance plateau allowing to expect a low thermal emittance, as confirmed by the high-temperature experiments

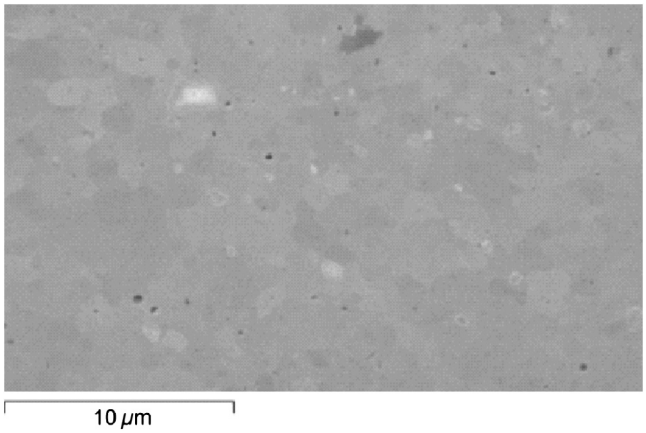

Fig. 1 Typical microstructure of dense HfB_2.

described below. On the contrary, SiC show a reflectance lower than 20% for wavelengths shorter than 10.5 μm and a single high-reflectance peak in the range 11 to 13 μm (about 90% reflectance), with a quickly decreasing reflectance for longer wavelengths (the reflectance is already dropped to about 40% at 14 μm). In the wavelength region of the solar spectrum (see inset of Fig. 2), SiC has a higher solar absorptivity, but the boride samples still are good absorbers (reflectance about 50% in the range 500 to 900 nm, where the sunlight spectral irradiance is maximum). The measured hemispherical reflectance $\rho'^{\cap}$ allows the calculation of the total solar absorbance α'_S according to the equation:

$$\alpha'_S = \frac{\int_{\lambda_{\min}}^{\lambda_{\max}} (1 - \rho'^{\cap}(\lambda)) \cdot S(\lambda) \mathrm{d}\lambda}{\int_{\lambda_{\min}}^{\lambda_{\max}} S(\lambda) \mathrm{d}\lambda}, \tag{1}$$

where $S(\lambda)$ is the sunlight spectrum,[13] with integration bounds $\lambda_{\min} = 0.3$ μm, $\lambda_{\max} = 2.3$ μm. The obtained values of α'_S for the two borides are very similar (0.49 for ZrB_2 and 0.48 for HfB_2, while α'_S for SiC is 0.78. However, the important parameter for solar absorber application is the absorbance-over-emittance ratio. From the acquired spectra, it is possible to estimate the emittance as

$$\varepsilon'(T) = \frac{\int_{\lambda_m}^{\lambda_M} [1 - \rho'^{\cap}(\lambda, T)] \cdot B(\lambda) \mathrm{d}\lambda}{\int_{\lambda_m}^{\lambda_M} B(\lambda) \mathrm{d}\lambda}, \tag{2}$$

being $B(\lambda)$ the blackbody irradiance at the considered temperature. From the experimental spectra, $\lambda_m = 0.3$ μm, $\lambda_M = 14.0$ μm. For example, for $T = 1400$ K, the calculated α'_S/ε' ratio is about 2 for ZrB_2, about 2.5 for HfB_2, and about 1 for SiC.

Table 1 Investigated samples.

Sample	Surface roughness (μm)	
ZrB_2	~0.04	Samples for spectral characterization
HfB_2	~0.02	
SiC	~0.04	
ZrB_2	0.3	Samples for emittance characterization
HfB_2	0.4	
SiC	0.3	

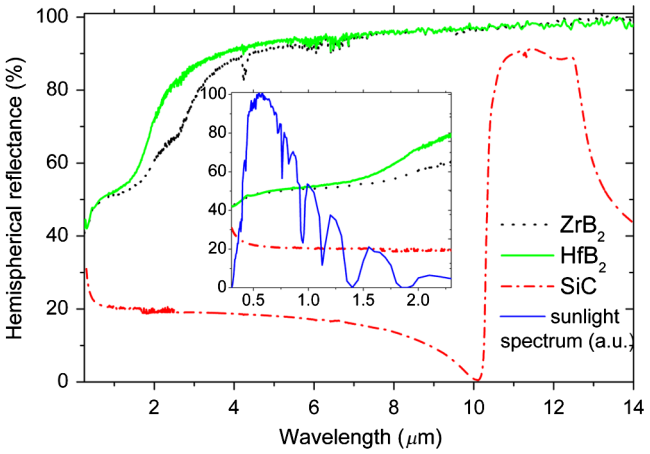

Fig. 2 Reflectance curves of almost fully dense ZrB_2, HfB_2, and SiC samples.

The measured total hemispherical emittance at high temperature is shown in Fig. 3. The favorable emittance characteristics of borides over SiC are immediately evident, as we obtained for HfB_2 and ZrB_2 and hemispherical emittance about a half of that of SiC. The two investigated borides show similar emittance values. A similar temperature dependence of emittance among ZrB_2 and HfB_2 can be inferred in the temperature region where the measurement ranges on the two samples are superimposed. Moreover for HfB_2, which has been investigated up to 1636-K temperature, the maximum measured emittance value is as low as 0.47. The obtained results show that boride UHTCs are promising for novel solar absorbers.

For a more comprehensive material characterization, the hemispherical emittance of samples has been investigated also in different spectral bands. The measurement has been carried out putting suitable spectral filters in front of the detector.

The experimental hemispherical emittance $\varepsilon_{\lambda 1,\lambda 2}(T)$ in a given $(\lambda 1, \lambda 2)$ range is defined as

$$\varepsilon_{\lambda 1,\lambda 2}(T) = \frac{\int_{\lambda 1}^{\lambda 2} I(\lambda, T)\mathrm{d}\lambda}{\int_{\lambda 1}^{\lambda 2} I_B(\lambda, T)\mathrm{d}\lambda}, \tag{3}$$

where the numerator is the hemispherical irradiance emitted by the sample at the temperature T, measured in the wavelength range $(\lambda 1, \lambda 2)$, and the denominator is the blackbody irradiance at the same temperature and in the same spectral interval. From the definition arises that $\varepsilon_{\lambda 1,\lambda 2}(T)$ gives information about the spectral shape of the radiance emitted by the sample, as compared with that emitted by a blackbody at the same temperature. In the gray body hypothesis, i.e., when a sample emits light with the same spectral shape as a blackbody at the same temperature, the emittance $\varepsilon_{\lambda 1,\lambda 2}(T)$ is a constant for any $(\lambda 1, \lambda 2)$ values. Thus, the fact that $\varepsilon_{\lambda 1,\lambda 2}(T)$ is a function of the chosen $(\lambda 1, \lambda 2)$ range means that the sample does not behave as a gray body. Moreover, the fact that the relative relationships between emittance values measured in the various $(\lambda 1, \lambda 2)$ intervals are a function themselves of the temperature means that also the nongray characteristic of the body is a function itself of the temperature.

Figure 4 shows the temperature dependence of the emittance in the considered bands as a function of the temperature. For a visual evaluation of the relative weight of the different contributions of the various spectral bands to the whole wavelength range, we show in Figs. 5 and 6 the histogram of the hemispherical emissivity of the boride samples measured in the considered spectral bands. Abscissas in Figs. 5 and 6 correspond to the width of the spectral range relative to each measurement.

From the definition [Eq. (3)], the measured emittance in the range $(\lambda 1, \lambda 2)$ represents the mean emittance value in the considered range. Therefore, by comparing the relative values, measured in the different spectral bands, we can obtain information about the spectral dependence of the emittance curve, defined as the limit value of $\varepsilon_{\lambda 1,\lambda 2}(T)$ for $(\lambda 1, \lambda 2) \to 0$.

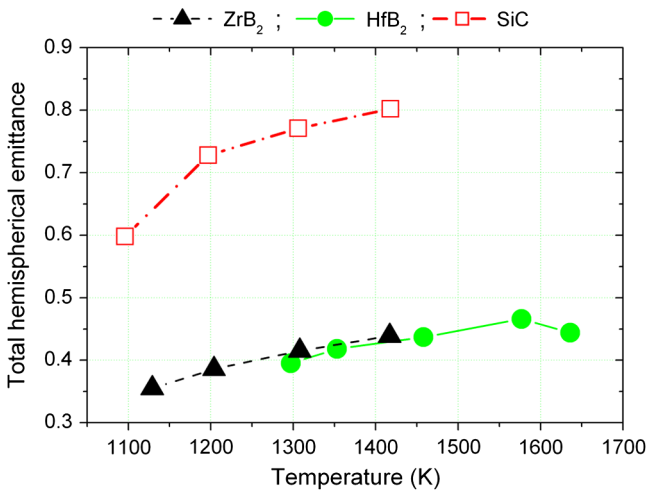

Fig. 3 Total hemispherical emittance of dense samples as a function of the temperature.

From Figs. 4–6, we can appreciate that the main contribution to the emittance is given by radiation emitted by the samples at wavelengths shorter than 2.8 μm, whereas at longer wavelengths, in the range 8 to 14 μm, the emittance is very low and considerably lower than the "total" 0.6- to 40-μm value. Therefore, as a general consideration, we can infer that borides have a spectral distribution of emitted light more peaked toward shorter wavelengths and with a lower long wavelength tail with respect to a blackbody at the same temperature. If we compare ZrB_2 and HfB_2, the emittances of the two samples are similar in all the investigated bands, with HfB_2 having a slightly lower emittance in the 8- to 14-μm wavelength range.

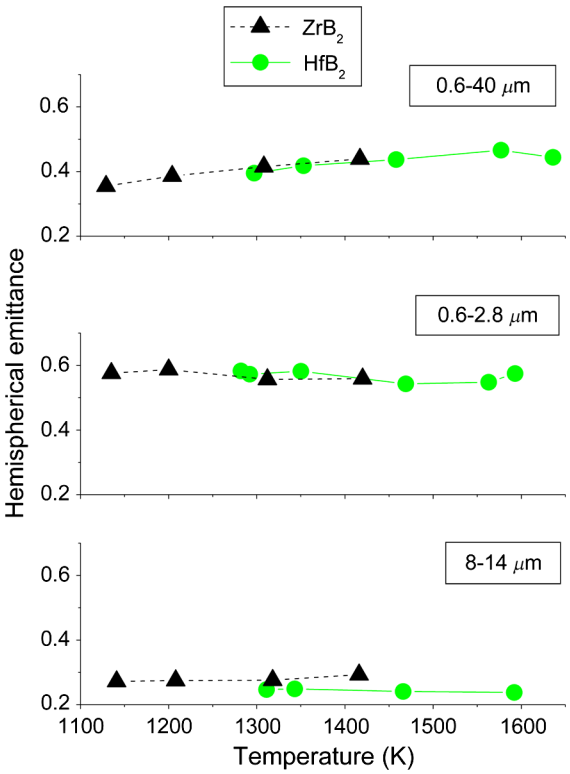

Fig. 4 Temperature dependence of the hemispherical emittance measured in the various spectral bands.

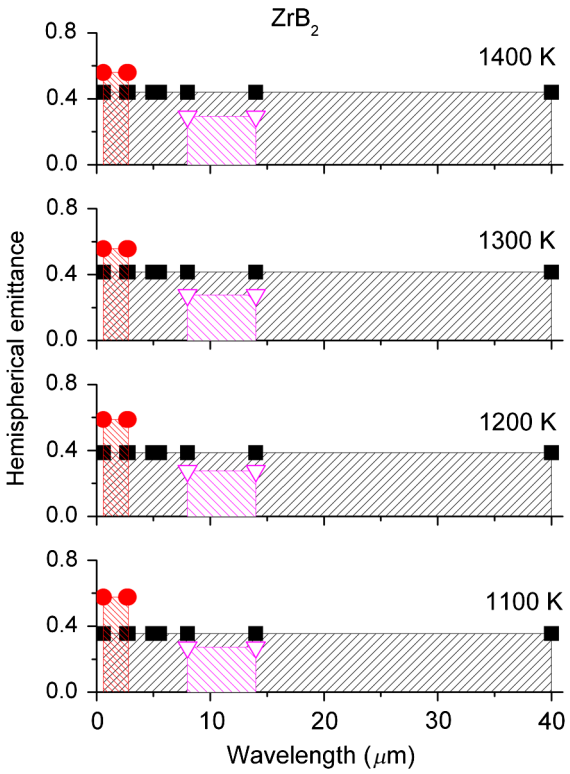

Fig. 5 Histogram of the measured emittance in the various bands for ZrB_2.

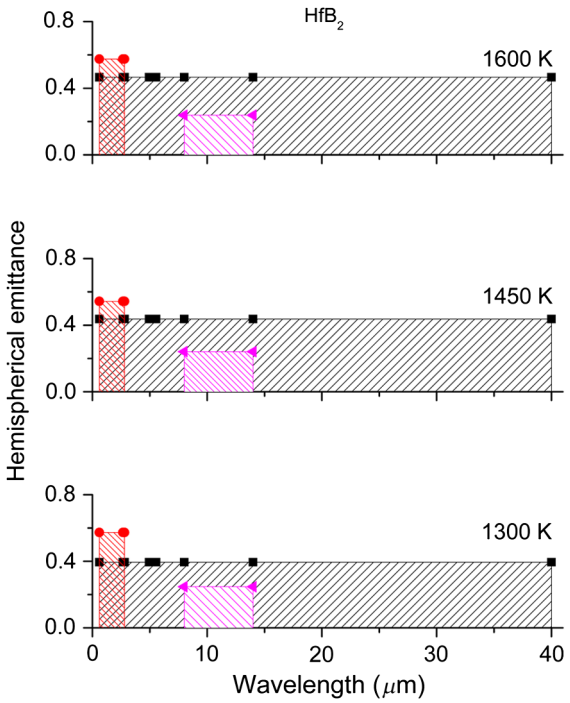

Fig. 6 Histogram of the measured emittance in the various bands for HfB_2.

As for the temperature dependence of the spectral band emission for both borides, as the temperature increases the emittance in the whole 0.6- to 40-μm range increases as well, while that in the bands 0.6 to 2.8 and 8 to 14 μm remains almost constant. This seems to suggest, as the temperature increases, a corresponding increase of the emission spectrum of samples in the 14- to 40-μm wavelength range, with an expected slightly larger increase for HfB_2 with respect to ZrB_2.

4 Conclusions

In this work, we report on the room-temperature spectral characterization in the wavelength range 0.3 to 14 μm and the high-temperature emittance properties of dense zirconium boride and hafnium boride UHTCs, in the perspective to use these materials as novel high-temperature solar absorbers in solar plants. Both the considered borides show good spectral selectivity properties and a thermal emittance considerably lower than that of silicon carbide, which is a material currently under development as solar absorber. High-temperature emittance measurements in different spectral bands allow to infer, for both borides, similar high-temperature spectra, with a blueshifted thermally emitted light with respect to the blackbody emission.

Acknowledgments

High-temperature measurements were possible with financial support by the Access to Research Infrastructures activity in the 7th Framework Programme of the EU (SFERA Grant Agreement n. 228296). Authors thank the PROMES Director and PROMES Researchers for the use of facilities. Thanks are due to Mauro Pucci, Massimo D'Uva, Roberto Rossi, and Leonardo Cirri for technical assistance.

References

1. W. G. Fahrenholtz et al., "Refractory diborides of zirconium and hafnium," *J. Am. Ceram. Soc.* **90**(5), 1347–1670 (2007), http://dx.doi.org/10.1111/jace.2007.90.issue-5.
2. E. Sani et al., "Ultra-refractory ceramics for high-temperature solar absorbers," *Scr. Mater.* **65**(9), 775–778 (2011), http://dx.doi.org/10.1016/j.scriptamat.2011.07.033.
3. E. Sani et al., "Hafnium and tantalum carbides for high temperature solar receivers," *J. Renewable Sustainable Energy* **3**, 063107 (2011), http://dx.doi.org/10.1063/1.3662099.
4. E. Sani et al., "Spectrally selective ultra-high temperature ceramic absorbers for high temperature solar plants," *J. Renewable Sustainable Energy* **4**, 033104 (2012), http://dx.doi.org/10.1063/1.4717515.
5. L. Silvestroni and D. Sciti, "Effects of MoSi2 additions on the properties of Hf- and Zr-B2 composites produced by pressureless sintering," *Scr. Mater.* **57**(2), 165–168 (2007), http://dx.doi.org/10.1016/j.scriptamat.2007.02.040.
6. D. Sciti et al., "Microstructure and mechanical properties of ZrB2-MoSi2 composites produced by different sintering techniques," *Mater. Sci. Eng. A* **434**(1–2), 303–306 (2006), http://dx.doi.org/10.1016/j.msea.2006.06.112.
7. D. Sciti, L. Silvestroni, and A. Bellosi, "Fabrication and properties of HfB2-MoSi2 composites produced by hot pressing and spark plasma sintering," *J. Mater. Res.* **21**(6), 1460–1466 (2006), http://dx.doi.org/10.1557/jmr.2006.0180.
8. D. Sciti et al., "Spark plasma sintering of HfB2 with low additions of silicides of molybdenum and tantalum," *J. Eur. Ceram. Soc.* **30**(15), 3253–3258 (2010), http://dx.doi.org/10.1016/j.jeurceramsoc.2010.06.006.
9. L. Silvestroni et al., "Transmission electron microscopy on Zr- and Hf-borides with MoSi2 additions," *J. Mater. Res.* **25**, 828–834 (2010), http://dx.doi.org/10.1557/JMR.2010.0126.
10. M. Balat-Pichelin et al., "Concentrated solar energy as a diagnostic tool to study materials under extreme conditions," *J. Solar Energy Eng.* **124**(3), 215–222 (2002), http://dx.doi.org/10.1115/1.1488164.

11. T. Paulmier et al., "Physico-chemical behavior of carbon materials under high temperature and ion irradiation," *Appl. Surf. Sci.* **180**(3–4), 227–245 (2001), http://dx.doi.org/10.1016/S0169-4332(01)00351-8.
12. T. Paulmier, M. Balat-Pichelin, and D. Le Quéau, "Structural modifications of carbon–carbon composites under high temperature and ion irradiation," *Appl. Surf. Sci.* **243**(1–4), 376–393 (2005), http://dx.doi.org/10.1016/j.apsusc.2004.09.106.
13. "Solar Spectral Irradiance," Technical Report no. 85, CIE (Commission Internationale de l'Eclairage), Wien (1989)

Biographies of the authors are not available.